Experiments on the Stability of the Flat-Plate Boundary Layer with Suction

G.A. Reynolds* and W.S. Saric†
Virginia Polytechnic Institute and State University, Blacksburg, Virginia

Experiments have been conducted in the Virginia Polytechnic Institute and State University Stability Wind Tunnel on a flat plate fitted with porous suction panels. Detailed hot-wire measurements were conducted in the laminar boundary layer to investigate the stabilizing effects of suction on the growth of Tollmien-Schlichting waves, which were introduced into the boundary layer using a vibrating ribbon. Special care was taken to minimize external disturbances and to avoid extraneous experimental bias. The measurements, which included mean-flow and disturbance-amplitude profiles across the boundary layer, showed that suction applied through discrete porous strips can be as effective as suction applied continuously over a much longer streamwise length. The measurements also showed that suction is more effective when placed forward, nearer to the region of neutral stability, than when placed in the region of maximum growth rate. These results also provided meaningful comparison with recent theory.

Nomenclature

$A(x)$	= disturbance-amplitude function; integrated amplitude of the Tollmien-Schlichting wave: [Eq. (1)]
C_p	= pressure coefficient, $=2(p-p_\infty)/\rho U_\infty^2$
F	= dimensionless frequency, $=(2\pi\nu f/U_\infty^2)\times 10^6$
f	= dimensional frequency, Hz
p	= static pressure
R	= Reynolds number based on δ_r, $=U_\infty\delta_r/\nu=R_x^{1/2}$
Re'	= unit Reynolds number, $=(U_\infty/\nu)\times 10^{-6}$/m
R_x	= Reynolds number based on x, $=U_\infty x/\nu$
R_I, R_{II}	= neutrally stable Reynolds numbers R for branches I and II
U_∞	= freestream velocity
u,v	= mean boundary-layer velocity along x and y
$\lvert u'\rvert, \lvert v'\rvert$	= rms of fluctuating velocity along x and y
v_0	= suction velocity
x,y,z	= rectangular coordinates along the streamwise, normal, and spanwise directions, respectively
δ	= boundary-layer thickness, $=5\delta_r$
δ_r	= boundary-layer reference length, $=(\nu x/U_\infty)^{1/2}$
η	= boundary-layer variable in the direction normal to the wall, $=y/\delta_r$
ρ	= air density

I. Introduction

THE feasibility and effectiveness of viscous drag reduction in aircraft via laminar flow control (LFC) have been demonstrated over the last 30 years.[1] LFC acts to alter the mean-velocity profile in such a way that it is more stable with respect to Tollmien-Schlichting waves. The implementation of LFC involves proper wing design to minimize the inviscid instabilities due to crossflow and curvature, as well as efforts to control the viscous instability so that laminar flow can be extended to Reynolds numbers one or two orders of magnitude higher than otherwise possible. The most effective LFC method to date has been boundary-layer suction applied through a large number of spanwise suction slots on the wings. Full-scale, in-flight tests have been conducted employing a wing glove with suction slots.[2] These tests obtained an overall drag reduction of 25%.

One of the first controlled wind-tunnel experiments examining boundary-layer stability in the presence of suction slots was done by Kozlov et al.[3] They made detailed mean-flow and disturbance measurements over a single slot on a flat plate and showed a large reduction of the disturbance amplitude in the neighborhood of the slot.

Recent improvements in wing surface materials for suction have resulted in a trend away from the suction-slot configuration and toward several types of porous skin materials. These porous surfaces provide the needed surface quality without the extensive machining needed for the suction-slot configuration.

The goal of the present work was to provide experimental support for the development of theoretical capabilities needed to incorporate suction in an LFC aircraft design. Experimental evidence was needed to identify the important controlling parameters for optimum stabilization, whether suction was applied through discrete spanwise slots or porous strips. The experiments to be described here were conducted on a flat plate with porous suction panels. Detailed hot-wire measurements were conducted in the laminar boundary layer to investigate the stabilizing effects of suction on growing Tollmien-Schlichting (T-S) waves. These two-dimensional waves were introduced into the boundary layer using a vibrating ribbon. Suction through the two porous panels was applied to a number of discrete, porous suction-strip configurations that included the continuous distribution. The results showed details of the mean-flow and disturbance-amplitude behavior with suction. These experiments are described in Sec. II and the results are discussed in Sec. III.

II. Description of the Experiment

The experiments were performed in the Virginia Polytechnic Institute and State University Stability Wind Tunnel. The facility is a closed-loop tunnel having a 9:1 contraction ratio to the test section which is 1.83 m square and 7.31 m long. Seven

Presented as Paper 82-1026 at the AIAA/ASME Third Joint Thermophysics, Fluids, Plasma and Heat Transfer Conference, St. Louis, MO, June 7-11, 1982; received July 22, 1982; revision received April 26, 1985.

*Research Associate, Department of Engineering Science and Mechanics; presently with: Advanced Research Organization, Lockheed-Georgia Company, Marietta, GA. Member AIAA.

†Professor, Department of Engineering Science and Mechanics; presently with: Department of Mechanical and Aerospace Engineering, Arizona State University, Tempe, AZ. Associate Fellow AIAA.

turbulence damping screens, having an open-area ratio of 0.6, are located in the settling chamber. The flow is driven by a 4.3-m-diam fan with eight constant-pitch blades. Turning vanes are located at each corner of the flow loop and those vanes located in the settling chamber are spaced every 0.076 m to help reduce any large-scale turbulence in the flow. The resulting flow in the test section is very uniform and steady, with a turbulence level of $|u'| = 0.02\% U_\infty$ at velocities of 16 m/s.

The experiments were conducted on a flat-plate model having a 1.83-m span, 3.66-m chord, and 0.021-m thickness. The model was a laminated panel that consisted of a 19-mm paper honeycomb core sandwiched between two 1-mm 6061-T6 aluminum sheets. This design was chosen for its light weight, strength, and very flat surface that was insensitive to temperature and humidity changes. A carefully contoured leading edge was used which had an elliptical profile with a major-to-minor axis ratio of 67:1. Chordwise and spanwise static pressure measurements were made with a total of 77 static pressure ports imbedded in the surface of the plate along one chordwise and two spanwise arrays. Differential pressures were measured via scanivalves and a ± 0.5-mm-Hg differential-pressure transducer. The pressure over the length of the plate deviated from zero pressure gradient no more than $\Delta C_p = \pm 0.5\%$, except near the leading- and trailing-edge regions. Local pressure gradients were always less than $dC_p/dx = 4 \times 10^{-3}$/m.

As shown in Fig. 1, the flat plate was constructed to accommodate four suction panels having 0.3-m chord and 0.91-m span. In these experiments, porous-surface panels were located at positions 1 and 2, whereas solid-surface panels were located at positions 3 and 4. The test surfaces of the model and leading edge were carefully polished to a rms surface roughness of 10 μm. Special care was taken at the leading-edge junction and around the panels to provide flat continuous surfaces. A contoured variable-deflection trailing-edge flap was used to control the position of the attachment line on the leading edge. In the absence of suction, transition was found aft of the porous panels at $R_x = 3.4 \times 10^6$. Transition was defined as the chordwise location where the sign of du/dx at fixed y changed from negative to positive. The details are contained in Refs. 4 and 5.

The porous-panel surface material, Dynapore, is a woven stainless-steel material of 80×700 mesh with an 80×80 mesh backing layer. Two porous panels were used in the suction experiments and these were designed and constructed based on the work of Pearce.[6] A chordwise cross-sectional view of the porous-panel assembly is shown in Fig. 2. Utilizing the spanwise flute construction, the suction distribution was varied on each panel from continuous suction over 254 mm to "discrete" suction of one 16-mm-wide strip. The total suction mass flow rate itself was held constant by an in-line sonic choking nozzle that also acted to isolate the panels from acoustic disturbances from the vacuum system.

The introduction of controlled disturbances into the boundary layer was accomplished using the vibrating-ribbon technique. The vibrating span of the ribbon was generally 0.4 m and was located above the plate surface, a distance $y/\delta_r = 0.17$ in boundary-layer coordinates. Careful placement of the ribbon made it possible to operate at freestream velocities of $U_\infty = 15$-20 m/s without exciting a flow-induced vibration of the ribbon. Measurements of ribbon amplitude and phase were accomplished by means of an inductance probe flush-mounted on the surface of the plate beneath the ribbon. These diagnostic measurements in the wind tunnel were combined with more detailed laboratory experiments to precisely determine the various vibrational characteristics of the ribbon. These characteristics were especially important when nonlinear vibrational response of the ribbon could be confused with nonlinear disturbance behavior in the boundary layer. It was also found that the ribbon could easily be excited in its torsional mode if special care was not taken in tensioning and clamping the ribbon.

Extensive measurements of mean and fluctuating velocities within the laminar boundary layer were conducted along the midspan of the plate using hot-wire anemometry in conjunction with a two-dimensional remotely controlled traversing mechanism. Computer control of the traversing mechanism and data-acquisition system allowed consistent and efficient collection of mean, rms, and spectral velocity information. Further details concerning the freestream flow quality and boundary-layer two-dimensionality are documented in Ref. 4.

The local pressure disturbance due to the traversing mechanism and the associated anemometer interference effects were evaluated first by surface static-pressure measurements. Local traverse blockage effects were minimized such that traverse-strut-mounted probes were well within the zero pressure gradient region ahead of the traverse. This was validated by observing the sensitivity of Tollmien-Schlichting waves to traverse motion. The disturbance wave amplitude, as measured by a fixed anemometer, did not change as a traverse-strut-mounted probe was moved upstream to a position corresponding to that of the fixed probe. These measurements demonstrated that two-dimensional T-S waves could be generated, allowed to grow, and be measured within a zero pressure gradient boundary layer, without interference from the traversing mechanism.

III. Procedures and Results

The basic state of the flat-plate experiment was established by the verification of zero pressure gradient and the determination of a high-transition Reynolds number. Verification of the stability experiment for the Blasius boundary layer was the foundation for extended work and this was established through measurements of the neutral stability points as a function of Reynolds number and frequency. Those results agreed very well with linear stability theory and previous experiments.

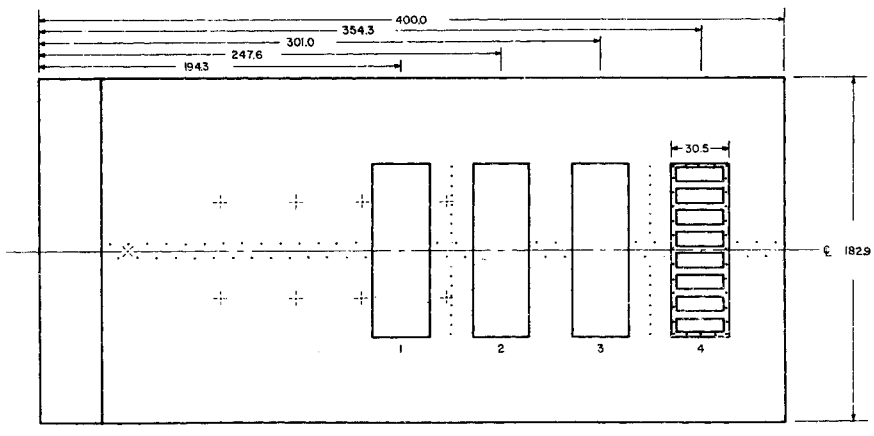

Fig. 1 Flat-plate suction model (without trailing-edge flap) showing porous panel locations as well as pressure ports •, inductance probe for ribbon monitoring ⊛ and smoke wire locations for flow visualization ⊕. Panel location 4 shows manifold arrangement on the back surface of the plate. Distances shown in centimeters from the leading edge.

Further details concerning those comparisons are contained in Ref. 5. Throughout the experiment special care was taken to minimize external disturbances in the flow and to ensure that only two-dimensional linear disturbances were introduced (see, for example, Ref. 7).

Since pressure gradient effects were present ahead of the vibrating ribbon, near the leading edge, it was necessary to establish a virtual leading-edge position for the Blasius boundary layer. At each measurement station, detailed mean-velocity profiles were used to determine the local Reynolds number R based on the measured reference length δ_r. This procedure ensured that the appropriate Reynolds number was established at each streamwise measurement station.

Throughout the series of tests, the total suction flow rate was kept constant at 10^{-3} m^3/s. This provided a range of suction velocities of $v_0 \cong 2.4\times10^{-3}$ m/s for spatially continuous suction over both panels to $v_0 \cong 73\times10^{-3}$ m/s for suction through a single suction strip. The available suction flow was divided almost equally between the two suction panels, depending only slightly on the number of strips opened on each panel.

In establishing the appropriate test conditions for the experiments, a number of factors were considered. While suction may have dramatic effects in the low Reynolds number region of the stability curve, in particular with regard to the minimum critical Reynolds number, it was recognized that high-frequency, low Reynolds number measurements do not have practical importance. Therefore, the experiments were conducted at the relatively low dimensionless frequencies of $F=20$ and 25, where $F=(2\pi\nu f/U_\infty^2)\times10^6$. Disturbances in this frequency range exhibit growth over a relatively large range of Reynolds numbers, from approximately $R_I \cong 900$ to $R_{II} \cong 2300$. Linear waves in this region experience a total growth of approximately $\ell n(A/A_0)=12$, where A_0 is the wave amplitude at the Branch I neutral stability point. Suction may then be applied in the region between R_I and R_{II} with the objective of limiting the wave growth, preferably keeping amplitudes in the linear regime, $|u'|/U_\infty \leqq 1\%$,

Seven test cases were conducted where suction was distributed in the region of growth for waves at $F=20$ or 25. These test cases are listed in Table 1 and described by Fig. 3, which shows the porous-panel locations relative to the unstable region from R_I to R_{II}. These relative porous-panel locations depended on the unit Reynolds number of the test.

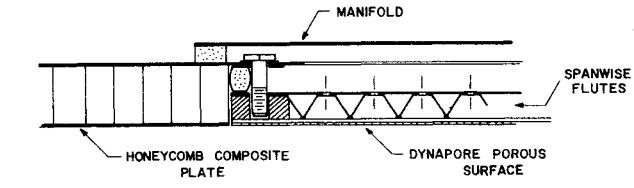

Fig. 2 Cross-section of porous-panel construction and assembly in the model.

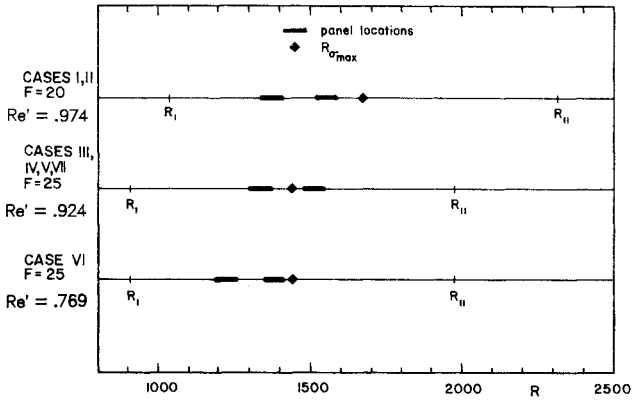

Fig. 3 Suction-panel placement relative to the neutral stability curve for seven suction cases. The maximum growth rate is at $R_{\sigma_{max}}$.

Table 1 Seven suction test cases and corresponding suction-strip configurations

Case No.	Frequency, F	Unit Reynolds No., Re'	No. of strips opened Panel 1	Panel 2
I	20	0.974	0	1
II	20	0.974	1	0
III	25	0.924	1	0
IV	25	0.924	3	3
V	25	0.924	7	3
VI	25	0.769	7	3
VII	25	0.924	15	15

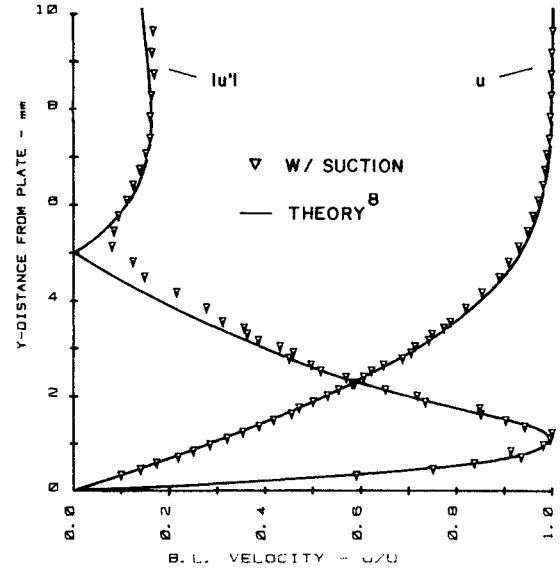

Fig. 4 Comparison of theory and experiment *with suction*. Data at $R=1376$ from test case III. A single suction strip is located at $R=1339$ with $v_0=5.7\times10^{-3}U_\infty$.

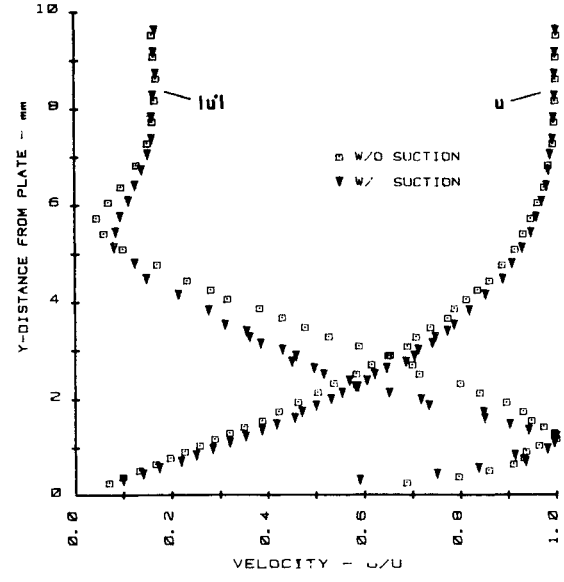

Fig. 5 Effects of suction on the mean- and disturbance-velocity profiles when compared to the no-suction data. Both disturbances profiles are normalized to 1.

The mean-flow and disturbance measurements for these experiments were obtained by a single hot-wire probe traversed across the boundary layer by the two-dimensional traverse. Typically, these measurements included mean velocity u, rms disturbance velocity $|u'|$, and the relative phase ϕ, where the phase is referenced to the vibrating-ribbon voltage. The ribbon in this case was 1.20 m from the leading edge. Examples of these data taken with and without suction are shown in Figs. 4 and 5. These profiles were obtained downstream of a single suction strip located at $x=1.94$ m. The suction velocity was $v_0=5.7\times10^{-3}U_\infty$ at a freestream velocity of 15 m/s. Measurements in the absence of suction, taken 2.05 m from the leading edge, showed good agreement between the mean-flow theory and experiment. The solution of the Orr-Sommerfeld equation in this case also showed good agreement between theory and experiment for the disturbance-amplitude distribution. In the case with suction, shown in Fig. 4, the theory of Reed and Nayfeh[8] is compared with the data for both the mean and disturbance flows. The maximum disturbance amplitude was 0.1% and was used to normalize the data. The agreement is very good. When a composite of the no-suction and suction data is formed, as shown in Fig. 5, we observe a slight filling of the mean-velocity profile that is characteristic of the role of suction. A more pronounced distortion of the normalized disturbance profile is observed as the disturbance energy is redistributed toward the wall to a region of higher dissipation. Both of the disturbance profiles have been normalized so that their maxima are unity. The unnormalized data show the amplitude of the no-suction case to be over three times the amplitude of the suction case.

The behavior of growing T-S waves under the influence of suction will now be described. With the traverse control and hot-wire measurements handled by the computer, it was possible to obtain much more detailed information of the disturbance amplitude and phase distribution at each streamwise station in the boundary layer. Because of this capability, the disturbance amplitude at a given streamwise station was expressed in terms of the integral of $|u'|$ across the boundary layer by

$$A(x)=\int_0^\infty \frac{|u'(x,y)|}{U_\infty}\,dy \tag{1}$$

This integration was carried out to the point of phase reversal since, by continuity and the fact that the phase is relatively constant except for the 180-deg shift at $|u'|=0$, this area must be equal to the area beyond the point of phase reversal. Integration of the disturbance profile provided a more complete evaluation of the disturbance amplitude than the usual single-point measurements for a number of reasons. First, the nonparallel effects in the boundary layer were minimized when compared with single-point measurements conducted along constant y or constant η (see, for example, Refs. 9 and 10). In addition, the experimental errors inherent in a single-point measurement were reduced by integration of the disturbance profile. Finally, profile integration allowed profile shape changes due to suction to be included in the measurement.

The experimental results obtained with various suction configurations were compared with the recent theory of Reed and Nayfeh.[8] This theory involves the use of a three-layer, or triple-deck, model of the boundary-layer flow with suction strips. The resulting linearized equations used the dimensionless suction level at each strip as a small parameter. Closed-form solutions describing the boundary-layer flow were then obtained. The solutions consisted of a mean flow, Blasius flow, and linearly superposed corrections due to each strip. Using these solutions for the streamwise velocity components, stability calculations were performed to obtain the disturbance behavior.

In all of the following plots, the disturbance amplitude at each station has been expressed in terms of the integrated streamwise rms component, Eq. (1). The resulting values have been normalized to the initial or lowest Reynolds number measurement, $A(x_0)$. In all cases, the initial disturbance amplitude in terms of the maximum of the disturbance profiles (near $\eta=1$) was $|u'|\cong0.05\%U_\infty$.

The disturbance-amplitude behavior for the single-strip suction configuration of test case III as a function of Reynolds number is shown in Fig. 6. Good agreement exists with the linear stability calculations for the Blasius data. In this test

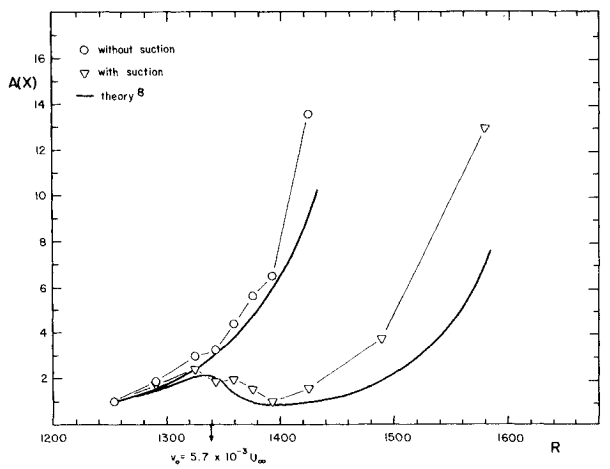

Fig. 6 Disturbance-amplitude function vs Reynolds number. Results for suction case III: $F=25$, $Re'=0.924$.

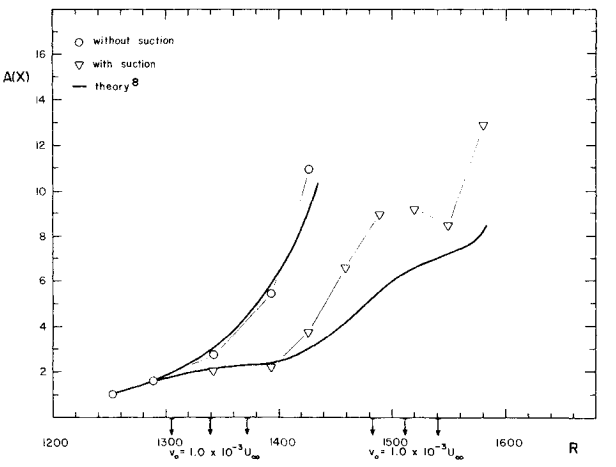

Fig. 7 Disturbance-amplitude function vs Reynolds number. Results for suction case IV: $F=25$, $Re'=0.924$.

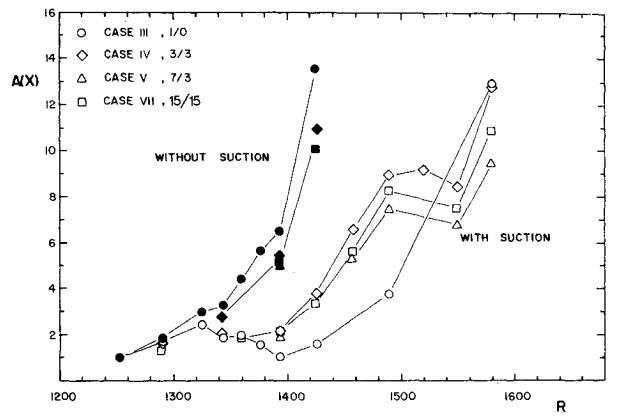

Fig. 8 Disturbance-amplitude function vs Reynolds number. Results for suction cases III, IV, V, and VII superposed: $F=25$, $Re'=0.924$.

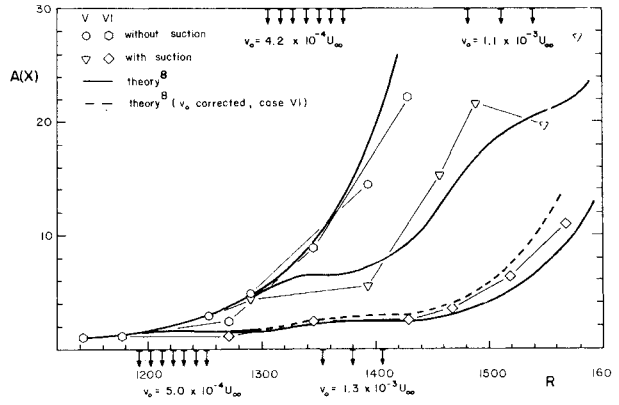

Fig. 9 Disturbance-amplitude function vs Reynolds number. Results for suction cases V and VI superposed: $F = 25$, $Re' = 0.924$ and 0.769. Corresponding suction-strip locations for cases V and VI are shown on the upper and lower horizontal axes, respectively.

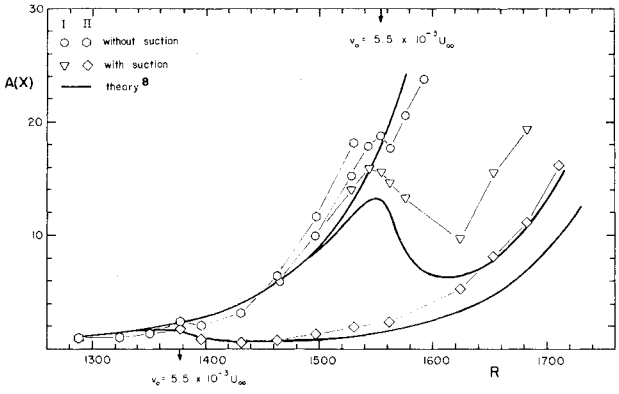

Fig. 10 Disturbance-amplitude function vs Reynolds number. Results for suction cases I and II superposed: $F = 20$, $Re' = 0.974$. The corresponding suction-strip locations for cases I and II are shown on the upper and lower horizontal axes, respectively.

case, suction through a single strip of $v_0 = 5.7 \times 10^{-3}\ U_\infty$ was intense enough to stop the disturbance growth and cause decay over a region beginning ahead of the suction strip and extending approximately 20δ downstream of the suction strip. In this case, the theory predicted a slightly greater downstream influence than the disturbance actually displayed, however, this suction level is considered to be quite large. The single-slot measurements of Kozlov et al.[3] were conducted at $F = 112$ and $R \cong 560$ with $v_0 = 0.14 U_\infty$. Thus, no experimental or theoretical comparison with their results could be made.

Keeping the overall mass-flow rate constant, the effect of multiple suction-strip configurations was tested in test cases IV-VII. In case IV, suction was applied through six suction strips, three on panel 1 and three on panel 2, (3/3). For case IV the suction velocity was $v_0 = 1 \times 10^{-3} U_\infty$, and the corresponding disturbance behavior is shown in Fig. 7. Compared to the single-strip case, a reduced upstream influence was observed ahead of the leading suction strips, with good agreement between theory and experiment over panel 1. As in case III, the agreement was not as good downstream of panel 1 where the theory predicted a slightly greater downstream influence.

The number of suction strips was increased again in suction cases V and VII, where the suction configurations on panels 1 and 2 were 7/3 and 15/15, respectively. The case with 15 strips opened on each panel was accomplished by opening all spanwise flutes, and so was a continuous suction case. The results of these multiple-strip cases were qualitatively similar to the 3/3 suction case already discussed. This is evident in Fig. 8 where all of the multiple-suction-strip cases at $F = 25$ and $Re' = 0.924$ are shown superposed along with the single-strip case III. In each of the three multiple-strip configurations, including continuous suction, the suction flow was divided almost equally between panels 1 and 2, where, in case III, the suction flow was concentrated through one strip on panel 1.

These results give some insight into the effect of various suction distributions on otherwise growing T-S waves. While it is apparent that suction becomes slightly more effective in cases V and VII as the distribution becomes more continuous, there is no general direction indicated as to the preferred suction distribution. The optimization scheme proposed by Reed and Nayfeh[8] suggested a preferred distribution of suction strips for a given suction mass-flow rate. The scheme minimized the total growth, $n = \ln(A/A_0)$, of a wave from branch I to branch II of the neutral stability curve. The results showed it to be preferable to concentrate suction in the initial region of growth near Branch I, and not at the region where the wave is most highly amplified. It was also suggested that any remaining suction be placed in the amplified region near Branch II.

The optimization scheme was tested directly by repeating the experiment of case V at the same dimensionless frequency of $F = 25$, and at the same suction mass-flow rate, but at a reduced unit Reynolds number. The resulting shift in the suction panel locations for case VI were shown in Fig. 3. The results of test case VI are shown superposed with the higher unit Reynolds number case V in Fig. 9. Here the relative suction-strip locations for cases V and VI have been indicated on the upper and lower horizontal axes, respectively. Agreement between theory and experiment is quite good here, with the theory accurately predicting the 55% reduction in disturbance amplitude from the aft-suction case to the forward-suction case.

The comparison drawn in Fig. 9 is not entirely complete; however, since the reduction of Re' in case VI caused a corresponding increase in the relative suction velocity v_0. However, this inconsistency in the comparison of cases V and VI resulted in only a very slight change in the disturbance behavior, as noted by the two theoretical curves shown for suction case VI. The dashed curve predicts the disturbance behavior if the suction flow had been reduced in case VI. To make the comparison of forward vs aft suction more complete, we may consider the two single-suction-strip cases I and II. In these cases, the suction mass-flow rate remained the same, but the tests were run at $F = 20$ and $Re' = 0.974$, as described in Table 1 and Fig. 3. The results of these two tests are shown combined in Fig. 10. The benefit of this fairly small shift forward of the suction strip can be readily observed. As in cases III and IV, the theory appears to overpredict the downstream effect of suction.

IV. Conclusions

Detailed mean-flow and disturbance-amplitude measurements have been conducted in a laminar boundary layer with suction applied through a number of porous suction-strip configurations. Measurements of the disturbance profile downstream of a single suction strip showed the profile distortion due to suction. The profile was shown to be moved toward the wall into a region of higher dissipation.

Experiments were conducted with a number of multiple-suction-strip configurations, including 3/3, 7/3 and 15/15 on panels 1 and 2, respectively. The relative merits of each were compared by maintaining the overall suction mass-flow rate constant throughout the test series. While the effect of suction in stabilizing the T-S waves was significant, the qualitative behavior of the data for these multiple-strip configurations varied only slightly from one configuration to the next. It is interesting to note that these comparisons showed the single-strip case III to be almost as effective as any of the multiple-strip cases.

The experimental and theoretical results have shown that the optimum forward vs aft-suction placement can be more

important than obtaining optimum interstrip spacing. The optimization scheme developed by Reed and Nayfeh[8] suggested that suction be concentrated not in the region of maximum growth rate, but further upstream in the weakly amplified region near branch I. The results of these experiments confirmed this hypothesis; assuming that suction not be concentrated forward at the expense of exceedingly high suction levels. Observed departures of the measured disturbance levels from the theoretical prediction in cases I-IV seem to suggest an upper limit on the acceptable suction velocity. Given that an upper ceiling is placed on the allowable suction velocity, the optimization scheme suggests that any remaining suction flow not used near branch I should be used in the region near branch II. This remains to be verified experimentally.

The generally good agreement between experiment and theory shows that the two-dimensional linear stability of the flat-plate boundary layer with suction can now be predicted. This holds for a wide class of suction distributions where the maximum suction velocity is held within prescribed levels.

Acknowledgments

The authors would like to express their thanks to Dr. H.L. Reed for her contribution of the theoretical results and to Mr. D.L. Weber for all of his valuable help in the experiment. The authors also acknowledge the encouragement, guidance, and support of Dr. W. Pfenninger and Messrs. D. Bushnell and J. Hefner. The porous panels were donated by the McDonnell Douglas Aircraft Company, Long Beach, CA. This work was supported by NASA Langley Research Center Grant NSG-1608.

References

[1]Pfenninger, W., "USAF & Navy Sponsored Northrop LFC Research Between 1949 and 1967," AGARD/VKI Special Course on Concepts for Drag Reduction, Rhode-St. Genese, Belgium, 1977.

[2]Pfenninger, W. and Groth, E., "Low Drag Boundary Layer Suction Experiments in Flight on a Wing Glove of an F-94A Airplane with Suction Through a Large Number of Fine Slots," *Boundary Layer and Flow Control*, Pergamon Press, New York, 1961, pp. 981-999.

[3]Kozlov, V.V., Levchenko, V.Ya., and Scherbakov, V.A., "Growth of Disturbances in a Boundary Layer with a Suction Slot," *Ucheniye Zapiski TsAGI*, Vol. 9, No. 2, 1978, pp. 99-105 (in Russian).

[4]Reynolds, G.A. and Saric, W.S., "Boundary-Layer Suction Experiments for Laminar Flow Control," Virginia Polytechnic Institute and State University, Blacksburg, VA., VPI-E-82.28, 1982.

[5]Saric, W.S. and Reynolds, G.A., "Laminar Flow Control Experiments on a Flat-Plate Boundary Layer," NASA-CR-157256, 1979.

[6]Pearce, W.E., "Application of Porous Materials for Laminar Flow Control," NASA CTOL Transport Technology Conference, McDonnell-Douglas Aircraft Company, Long Beach, CA., Douglas Paper 6693, 1978.

[7]Saric, W.S. and Reynolds, G.A., "Experiments on the Stability of Nonlinear Waves in a Boundary Layer," *Laminar-Turbulent Transition*, edited by R. Eppler and H. Fasel, Springer-Verlag, New York, 1980, pp. 125-134.

[8]Reed, H.L. and Nayfeh, A.H., "Numerical-Perturbation Technique for Stability of Flat-Plate Boundary Layers with Suction," *AIAA Journal*, Vol. 24, Feb. 1986, pp. 208-214.

[9]Gaster, M., "On the Effects of Boundary-Layer Growth on Flow Stability," *Journal of Fluid Mechanics*, Vol. 66, 1974, pp. 465-480.

[10]Saric, W.S. and Nayfeh, A.H., "Nonparallel Stability of Boundary Layers with Pressure Gradients and Suction," AGARD CP 224, 1977, pp. 6.1-6.20.